SUPPLEMENTAL FIGURE LEGENDS

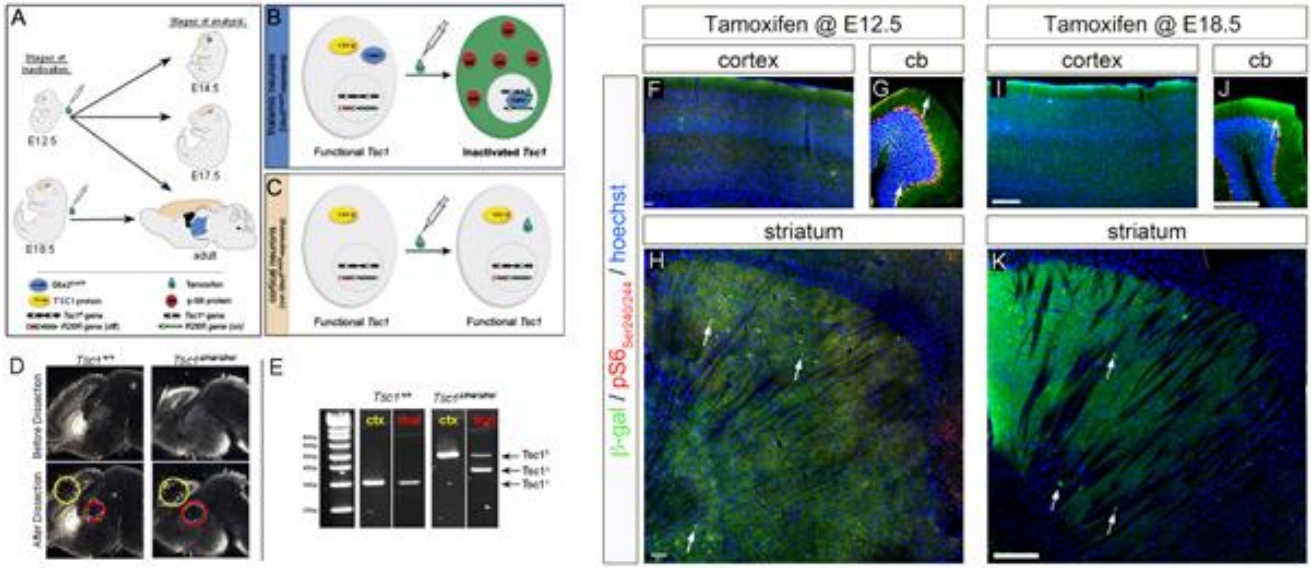

Figure S1, related to Figure 1. Spatial control over *Tsc1*^{fl} allele recombination. (A) Experimental approach. Tamoxifen is administered at E12.5 or E18.5, and animals are analyzed at E14.5, E17.5, or postnatally. Thalamus is shown in blue, cerebral cortex is in tan. (B) Within thalamic, *Gbx2*^{CreER}-expressing cells, tamoxifen activates the CreER protein (blue), allowing it to translocate into the nucleus, where it has access to the genome and where it mediates recombination of *loxP* sites (triangles), thereby deleting the *Tsc1*^{fl} allele (black) and activating the reporter allele (green). (C) In cells, such as cortical neurons, that do not express *Gbx2*^{CreER}, tamoxifen has nothing to act upon, so the *Tsc1*^{fl} allele remains functional and the reporter allele remains quiescent, despite being exposed to tamoxifen. (D) Control (*Tsc1*$^{+/+}$) and mutant (*Tsc1*$^{\Delta E12/\Delta E12}$) were harvested at E17.5. Sagittal brain sections (12□m) were manually microdissected to collect thalamic tissue (red circle) as well as control tissue from the cerebral cortex (yellow circle). (E) Tissue was lysed, and PCR was performed to detect the three alleles of *Tsc1*: *Tsc1*$^{+}$ (295bp), *Tsc1*^{fl} (486bp), and *Tsc1*$^{\Delta}$ (368bp). Conversion of the *Tsc1*^{fl} allele into the *Tsc1*$^{\Delta}$ allele is seen only in the thalamic tissue where *Gbx2*^{CreER} is expressed, but not in the cortical tissue, where there is no CreER expression. *Tsc1*$^{+}$ is unaffected in both the cortical and thalamic tissue samples, as expected. (F-H) IHC was performed on *Gbx2*^{CreER};*R26*^{LacZ};*Tsc1*$^{+/+}$ animals that received tamoxifen at E12.5 (F-H) or E18.5 (I-K). ß-gal labeling (green) indicates very sparse recombination within the cerebellum (arrows) and striatum and a lack of any recombination in the cortex. pS6 (red) shows that some of the ß-gal cells respond to *Tsc1* inactivation with mTOR dysregulation. Purkinje cells of the cerebellum express high basal levels of p-S6, regardless of recombination.

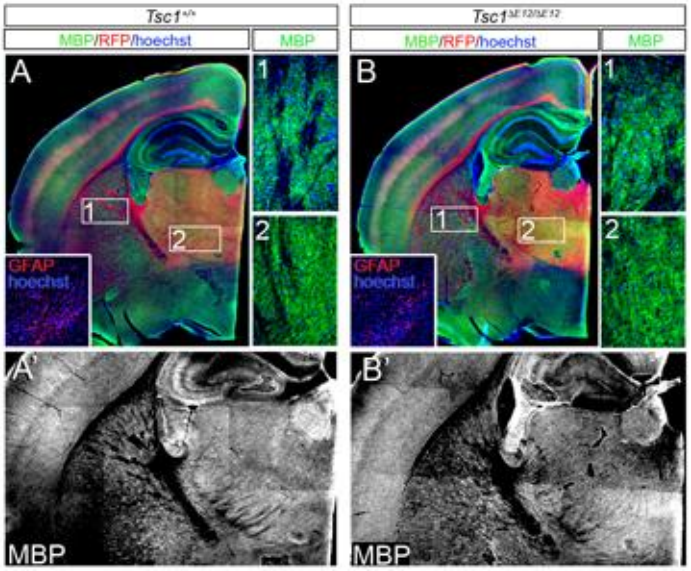

Figure S2, related to Figure 3. Astrocytes and myelination are unaffected in E12.5 *Tsc1*$^{\Delta E12/\Delta E12}$ mutants. (A, B) *Tsc1*$^{+/+}$ and *Tsc1*$^{\Delta E12/\Delta E12}$ adult brain sections were stained for myelin basic protein (MBP, green) and RFP (red). MBP staining is present throughout the brain, as expected, and there are no apparent differences between control and mutant staining patterns. High magnification panels show details of MBP labeling (green) within the internal capsule (region 1) and thalamus (region 2). Insets: IHC for GFAP (red), an astrocyte marker, was also performed on thalamic sections to determine if gliosis occurred as a result of early *Tsc1* inactivation. GFAP+ astrocytes were sparse in the thalamus, and no differences in staining were observed between control and *Tsc1*$^{\Delta E12/\Delta E12}$ thalamus. MBP is isolated and shown in black and white in A' and B'.

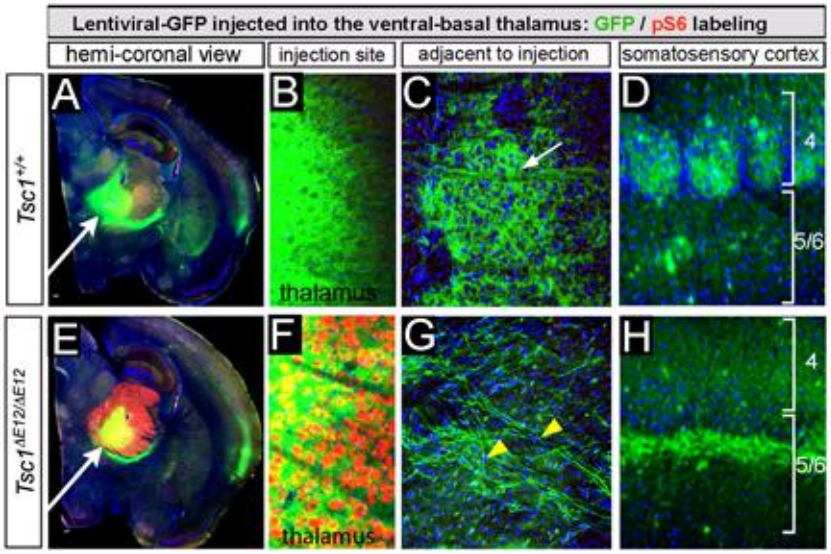

Figure S3, related to Figure 4. Altered distribution of thalamic projections in the internal capsule and cerebral cortex of *Tsc1*$^{\Delta E12/\Delta E12}$ mutants. Lentiviral-GFP was stereotactically injected into the ventrobasal region of the thalamus. After waiting two weeks for expression, the brains were harvested, sectioned, and immunostained for GFP (green) and pS6 (red). GFP+ thalamic axons can be seen exiting the control (A,B) or mutant thalamus (E,F), traversing the striatum (C,G), and entering the cerebral cortex (D,H). Characteristic whisker barrels of the somatosensory cortex can be clearly delineated by the preferential thalamocortical innervation in control brains (D), whereas this barrel pattern is much less apparent in the *Tsc1*$^{\Delta E12/\Delta E12}$ brain (H) and the GFP+ projections instead stratify in deeper cortical layers.

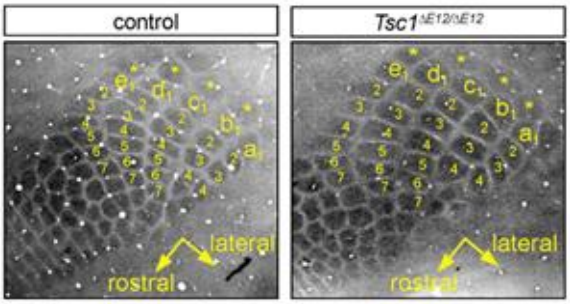

Figure S4, related to Figure 5. *Tsc1*$^{\Delta E18/\Delta E18}$ animals have normal whisker barrel structure. Tangential sections through layer IV somatosensory cortex and stained for cytochrome oxidase (black) shows well-organized barrel field in both control and *Tsc1*$^{\Delta E18/\Delta E18}$ mutant brains. Conventional vibrissae identifiers are indicated.

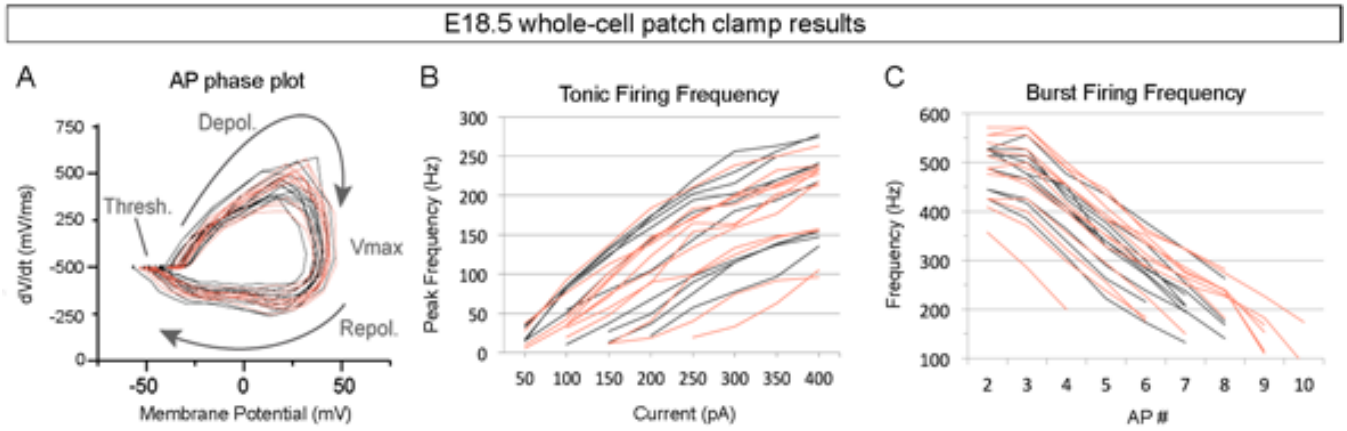

Figure S5, related to Figure 6. Whole-cell physiology of *Tsc1*$^{\Delta E18/\Delta E18}$ mutant thalamic neurons. (A) AP dynamics are shown in a phase plot for *Tsc1*$^{+/+}$ and *Tsc1*$^{\Delta E18/\Delta E18}$, similar to Figure 6C. There is no difference in any of the AP properties analyzed. (B) Peak firing frequency per current injection is plotted, similar to Figure 6F. *Tsc1*$^{\Delta E18/\Delta E18}$ VB neurons (pink lines) have firing frequency as *Tsc1*$^{+/+}$ neurons (gray lines). (C) Firing frequency per AP within a post-hyperpolarization rebound burst is plotted, similar to Figure 6I. There is no difference between the *Tsc1*$^{\Delta E18/\Delta E18}$ neurons and the *Tsc1*$^{+/+}$ neurons. See Table S1 for means and statistics.

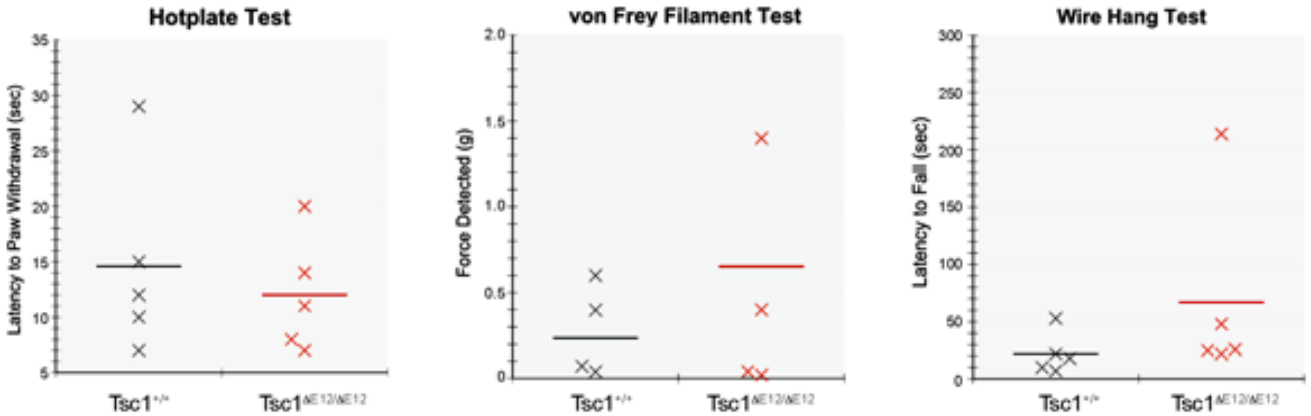

Figure S6, related to Figure 7. Sensory and motor function is unaffected in *Tsc1*$^{\Delta E12/\Delta E12}$ mice. Sensory perception and motor function in *Tsc1*$^{\Delta E12/\Delta E12}$ mice and their littermate controls were compared using the hotplate test, von Frey filaments, and a wire hang assay to test thermal pain sensitivity, tactile

sensitivity, and motor function, respectively. *Tsc1*$^{\Delta E12/\Delta E12}$ (n=5) did not differ significantly from control animals (n=5) in any of the assays (two-tailed t-tests, $p>0.05$), indicating that their sensorimotor functions are not compromised. Data points indicate performance level for individual mice. Horizontal lines indicate population means.

Supplemental Video 1, related to Figure 7. *Tsc1*$^{\Delta E12/\Delta E12}$ mouse is shown during a typical seizure. Note that seizure begins with clasping of the hindpaw, then loss of upright posture resulting in a twisting convulsive motion. Afterwards, upright posture is regained and, after a brief pause, normal activity is resumed.

Supplemental Video 2, related to Figure 7. Rare, handling-induced seizure in a *Tsc1*$^{\Delta E18/\Delta E18}$ animal is shown. Immediately prior to start of video, mouse was picked up by the tail and replaced into the homecage. Note that these handling-induced seizures do not have the characteristic twisting posture common to the spontaneous *Tsc1*$^{\Delta E12/\Delta E12}$ seizures.

Table S1. Mean Values, Sample Sizes, and Statistical Analysis of Cellular Properties

Property	Tamoxifen	Genotype	number of cells	mean	geometic mean	s.e.m. (lower)	s.e.m. (upper)	95% CI (lower)	95% CI (upper)	p value (if adjusted, with Holm)
Soma area (mm^2)	E12.5	Tsc1+/+ (pS6-)	1061		220.02	-1.96	1.97	211.73	228.62	
	E12.5	Tsc1DE12/+ (pS6-)	1068		209.47	-1.86	1.88	201.58	217.69	0.181 (adj.)
	E12.5	Tsc1DE12/DE12, (pS6-)	257		203.73	-3.66	3.73	188.45	220.26	**0.003 (adj.)**
	E12.5	Tsc1DE12/DE12, (pS6+)	621		403.51	-4.67	4.73	383.77	424.24	**0.004 (adj.)**
	E18.5	Tsc1+/+ (pS6-)	630		253.36	-16.53	17.67	204.42	314.00	n.d.
	E18.5	Tsc1+/+ (pS6+)	2		304.81	n.d.	n.d.	n.d.	n.d.	
	E18.5	Tsc1DE18/+ (pS6-)	1061		242.38	-17	18.28	192.30	305.45	0.142 (adj.)
	E18.5	Tsc1DE18/+ (pS6+)	8		277.30	-33.1	37.58	185.03	415.59	
	E18.5	Tsc1DE18/DE18, (pS6-)	542		246.73	-16.09	17.22	199.06	305.82	0.110 (adj.)
	E18.5	Tsc1DE18/DE18, (pS6+)	221		358.53	-33.87	37.39	358.52	491.67	
Resting Membrane Potential (mV)	E12.5	Tsc1+/+	12	-61.81		-0.43	0.43	-62.81	-60.82	**0.006**
	E12.5	Tsc1DE12/DE12	18	-58.06		-0.92	0.92	-60.17	-55.94	
	E18.5	Tsc1+/+	12	-61.86		-0.94	0.94	-64.03	-59.70	0.155
	E18.5	Tsc1DE18/DE18	13	-60.14		-0.57	0.57	-61.46	-58.81	
Input Resistance (mW)	E12.5	Tsc1+/+	12		137.20	-15.648	17.662	103.76	181.15	**0.001**
	E12.5	Tsc1DE12/DE12	18		72.59	-3.098	3.236	65.64	80.27	
	E18.5	Tsc1+/+	12		157.75	-15.14	16.748	125.01	199.06	0.318
	E18.5	Tsc1DE18/DE18	13		132.22	-16.292	18.583	97.64	179.06	
Input Capacitance (pF)	E12.5	Tsc1+/+	12		219.66	-28.066	32.178	160.28	301.09	**0.004**
	E12.5	Tsc1DE12/DE12	18		417.63	-35.789	39.143	339.71	513.47	
	E18.5	Tsc1+/+	12		237.75	-30.397	34.853	173.45	325.40	0.439
	E18.5	Tsc1DE18/DE18	13		267.47	-12.303	12.896	239.94	298.15	
Membrane Time Constant (msec)	E12.5	Tsc1+/+	12		30.14	-4.252	4.951	21.22	42.80	0.958
	E12.5	Tsc1DE12/DE12	18		30.43	-2.787	3.068	24.39	37.98	
	E18.5	Tsc1+/+	12		37.51	-1.322	1.37	34.53	40.74	0.647
	E18.5	Tsc1DE18/DE18	13		35.03	-4.54	5.217	25.43	48.26	
Max AP Rise (mV/msec)	E12.5	Tsc1+/+	12		423.41	-11.86	11.86	396.07	450.76	**<0.001**
	E12.5	Tsc1DE12/DE12	18		618.44	-26.36	26.36	557.64	679.25	
	E18.5	Tsc1+/+	12		451.44	-19.06	19.06	407.50	495.38	0.478
	E18.5	Tsc1DE18/DE18	12		472.56	-21.01	21.01	424.10	521.02	
Max AP Fall (mV/msec)	E12.5	Tsc1+/+	12		-151.54	-12.69	12.69	-180.81	-122.27	**<0.001**
	E12.5	Tsc1DE12/DE12	18		-262.75	-8.39	8.39	-282.10	-243.40	
	E18.5	Tsc1+/+	12		-175.72	-5.36	5.36	-188.09	-163.35	0.603
	E18.5	Tsc1DE18/DE18	12		-182.88	-12.07	12.07	-210.71	-155.05	
AP amplitude (mV)	E12.5	Tsc1+/+	12		70.39	-1.72	1.72	66.43	74.36	**<0.001**
	E12.5	Tsc1DE12/DE12	18		82.40	-0.74	0.74	80.71	84.10	
	E18.5	Tsc1+/+	12		71.69	-0.66	0.66	70.17	73.21	0.135
	E18.5	Tsc1DE18/DE18	12		74.10	-1.29	1.29	71.13	77.06	
AP Half-width (msec)	E12.5	Tsc1+/+	12	0.43		-0.0234	0.0256	0.39	0.49	**0.002**
	E12.5	Tsc1DE12/DE12	18	0.32		-0.008	0.008	0.31	0.34	
	E18.5	Tsc1+/+	12	0.41		-0.016	0.016	0.37	0.44	0.955
	E18.5	Tsc1DE18/DE18	12	0.40		-0.022	0.024	0.35	0.46	
Peak fAHP Potential (mV)	E12.5	Tsc1+/+	11	-0.10		0.98	0.98	-2.37	2.17	**0.005**
	E12.5	Tsc1DE12/DE12	17	-4.24		0.45	0.45	-5.28	-3.21	
	E18.5	Tsc1+/+	11	-0.11		0.96	0.96	-2.31	2.10	0.871
	E18.5	Tsc1DE18/DE18	12	0.12		0.92	0.92	-2.00	2.23	
ADP+AHP area (mV)	E12.5	Tsc1+/+	11	-63.72		14.73	14.73	-97.70	-29.75	**0.003**
	E12.5	Tsc1DE12/DE12	17	-177.15		21.89	21.89	-227.63	-126.68	
	E18.5	Tsc1+/+	11	-81.95		9.60	9.60	-104.08	-59.82	0.623
	E18.5	Tsc1DE18/DE18	12	-69.86		21.60	21.60	-119.66	-20.06	
Tonic F/I slope (Hz*pA)	E12.5	Tsc1+/+	12	0.53		0.01	0.01	0.50	0.56	**<0.001**
	E12.5	Tsc1DE12/DE12	16	0.27		0.03	0.03	0.21	0.33	
	E18.5	Tsc1+/+	10	0.59		0.04	0.04	0.50	0.69	0.278
	E18.5	Tsc1DE18/DE18	12	0.52		0.04	0.04	0.42	0.62	
Peak Tonic Firing Frequency @ 200pA (Hz)	E12.5	Tsc1+/+	12	188.30		2.15	2.15	183.34	193.25	**0.001**
	E12.5	Tsc1DE12/DE12	16	120.74		12.41	12.41	92.13	149.35	
	E18.5	Tsc1+/+	10	210.30		17.02	17.02	171.05	249.55	0.557
	E18.5	Tsc1DE18/DE18	12	195.35		17.50	17.50	154.99	235.71	
Mean Intraburst Spike Frequency (Hz)	E12.5	Tsc1+/+	12	339.27		21.43	21.43	289.85	388.70	**0.026**
	E12.5	Tsc1DE12/DE12	18	400.89		7.03	7.03	384.68	417.09	
	E18.5	Tsc1+/+	10	355.99		12.16	12.16	327.95	384.03	0.585
	E18.5	Tsc1DE18/DE18	13	346.78		10.70	10.70	322.09	371.46	
# of spikes per burst	E12.5	Tsc1+/+	12		7.38	-0.704	0.778	5.86	9.30	0.409
	E12.5	Tsc1DE12/DE12	18		8.28	-0.682	0.744	6.79	10.10	
	E18.5	Tsc1+/+	10		7.27	-0.079	0.08	7.09	7.46	0.738
	E18.5	Tsc1DE18/DE18	13		7.43	-0.454	0.484	6.43	8.60	
Peak Burst Firing Frequency (Hz)	E12.5	Tsc1+/+	12		496.21	-29.0023	29.0023	429.33	563.09	0.514
	E12.5	Tsc1DE12/DE12	18		519.79	-18.681	18.681	476.71	562.87	
	E18.5	Tsc1+/+	10		493.73	-15.6677	15.6677	457.60	529.86	0.719
	E18.5	Tsc1DE18/DE18	13		485.54	-15.3921	-15.3921	450.04	521.03	

SUPPLEMENTAL EXPERIMENTAL PROCEDURES

Mice

Tsc1^{fl} (Kwiatkowski et al., 2002) and *R26*$^{loxP\text{-}STOP\text{-}loxP\text{-}tdTomato}$ (*R26*^{tdTomato}) (Madisen et al., 2010) mice were obtained from Jackson laboratories (stock # 005680 and #007905, respectively). *Gbx2*$^{CreER\text{-}IRES\text{-}eGFP}$ mice (*Gbx2*^{CreER}) (Chen et al., 2009) and *Rosa26*$^{loxP\text{-}STOP\text{-}loxP\text{-}LacZ}$ reporter (*R26*^{LacZ}) mice (Soriano, 1999) were generously provided by J. Li (UConn Health Center) and P. Soriano (Mt. Sinai School of Medicine), respectively. *Gbx2*^{CreER} mice were bred with *Tsc1*$^{fl/fl}$ mice and either *R26*^{LacZ} or *R26*^{tdTomato} mice to maintain a compound line. Genotyping was performed as previously described for the *CreER* and *R26*^{LacZ} alleles (Ellisor et al., 2009). Genotyping for the *R26*^{tdTomato} allele was performed as described on the jax.org website. Genotyping for the *Tsc1*$^{+}$, *Tsc1*^{fl}, and *Tsc1*$^{\Delta}$ allele was performed as previously described (Figure S1) (Kwiatkowski et al., 2002). *Tsc1*^{fl} inactivation experiments were conducted by crossing *Gbx2*^{CreER}*;R26*^{LacZ}*;Tsc1*$^{fl/+}$ or *Gbx2*^{CreER}*;R26*^{tdTomato}*;Tsc1*$^{fl/+}$ males with *Tsc1*$^{fl/+}$ females. The morning (0900) of the day a vaginal plug was detected was designated as embryonic day (E)0.5. 4mg of tamoxifen (20mg/mL in corn oil) was administered by oral gavage (Kwiatkowski et al., 2002; Brown et al., 2009)to the pregnant females harboring embryos at embryonic stage (E)12.5 or E18.5 to simultaneously activate the *R26*^{LacZ} or *R26*^{tdTomato} allele and induce recombination of the *Tsc1*^{fl} allele into the *Tsc1*$^{\Delta}$ allele within the embryos (Figure S1). Mice were housed and handled in accordance with Brown University Institutional Animal Care and Use Committee guidelines.

Tissue Processing, Immunohistochemistry (IHC), and cytochrome oxidase staining

For embryonic analysis, timed-pregnant females harboring embryos at the desired pregnancy stage (E14.5 or E17.5; n≥3 each stage and genotype) were sacrificed at 0900, the uterine chain was dissected out, embryos were genotyped, immersion-fixed in 4% paraformaldehyde (PFA), cryoprotected in 30% sucrose, frozen in Optimal Cutting Temperature (OCT, Fisher), and sectioned on a Leica cryostat as previously described (Ellisor et al., 2009; Madisen et al., 2010). For postnatal tissue analysis, animals were deeply anesthetized with 195mg/kg Beuthanasia-D (Schering-Plough Animal Health Corp.) and intracardially perfused. Craniotomies were performed as previously described (Brown et al., 2009; Chen et al., 2009). And brains were sectioned at a sagittal angle (40 µm) or a thalamocortical angle (60 µm) (Agmon and Connors, 1991; Soriano, 1999) using a Leica vibratome. Embryonic sections and adult free-floating sections were matched based on morphology and processed for IHC by standard methods (Ellisor et al., 2009) using primary antibodies raised against the following antigens: phosphorylated S6 ribosomal protein at Ser240/244 (pS6, rabbit, 1:800, Cell Signaling), phosphorylated S6 ribosomal protein at Ser235/236 (1:100, rabbit, Cell Signaling), ß-galactosidase (1:500, goat, Biogenesis or 1:500, chicken, Abcam), GFP (1:500, rat, Nacalai Tesque or 1:600, rabbit, Invitrogen), RFP (1:1000, chicken, VWR), , MAP-2 (1:500, mouse, Sigma), calbindin D-28K (1:1000, rabbit, Swant), parvalbumin (mouse, 1:1000, Sigma), myelin basic protein (MBP, rabbit, 1:500, Millipore), glial fibrillary acidic protein (GFAP, rabbit, 1:500, Millipore), Neuronal Nuclei (NeuN, mouse,1:500, Millipore). The following secondary antibodies from Invitrogen were used at a 1:500 dilution in 1% normal donkey serum/PBS-Triton X-100: Alexa 488 donkey anti-rabbit IgG, Alexa 555 donkey anti-rabbit IgG, Alexa 488 donkey anti-rat IgG, Alexa 555 donkey anti-goat IgG, and Alexa 488 donkey anti-mouse IgG (Molecular Probes) and DyLight 549 donkey anti-chick IgG (Jackson ImmunoResearch). All sections were counterstained using the Hoechst 33342 (Molecular Probes) and mounted on ColorFrost Plus Slides (Fisher) using Fluoromount-G mounting media (Southern Biotech).

For cytochrome oxidase (CO) staining of vibrissa barrels, mice were deeply anesthetized and intracardially perfused with 4% paraformaldehyde/1% glutaraldehyde in PBS. The brains were taken from the head and the two hemispheres were separated by a longitudinal cut along the midline. The cerebellum, brainstem, thalamus, hippocampus, olfactory bulb, temporal lobe and most of the subcortical white matter were removed. The two hemispheres were flattened between two glass slides in fix solution (4% PFA, 1% gluteraldehyde in PBS) for 1 hour at 4^{O}C. The flattened hemispheres were cryoprotected 30% sucrose solution at 4^{O}C, frozen in OCT, and sectioned on a Leica cryostat at 50µm (E12.5 samples) or 100µm (E18.5 samples). The sections were incubated with 5mg DAB (Sigma), 2mg Cytochrome C (Sigma), and 0.4g sucrose in 10mL PBS at 37^{O}C in the dark for 1-3 hours, washed with

PBS, and mounted on slides with Fluoromount-G. Adobe Illustrator was used for outlining the barrels stained with CO on different sections. The outlines from all of the barrel-containing sections were co-registered based on morphological landmarks and/or blood vessel locations, and collapsed to form a representative map of the full barrel field.

For neuron density analysis, a barrel outline was created based on CO+ staining ("barrel hollow") and a perimeter was made 15μm outside the inner outline ("barrel wall") using Adobe Illustrator's offset path function. The area and the number of NeuN-positive objects in the barrel hollow and wall regions were determined using the automated "measure area" and "find points" function in Volocity software (Improvision). Quantative barrel analysis was analyzed for significance by Student's t-test.

Microscopy and Cell Size Analysis

Sections were imaged on a Leica DM600B epifluorescent microscope with Volocity 5.1 imaging software (Improvision). Red, green, and blue channels were imaged separately and pseudocolored as part of the acquisition palettes. Identical exposure settings were used across the three genotypes to allow for direct comparison of labeling intensity. Post-acquisition image processing was performed in Adobe Photoshop, with control and experimental data processed identically. For cell size analysis, free-floating adult sagittal sections from *Tsc1*$^{+/+}$, *Tsc1*$^{fl/+}$ and *Tsc1*$^{fl/fl}$ animals (n=3 each genotype) were processed for IHC using primary antibodies to MAP-2 and p-S6$_{Ser240/244}$, as described above. Five thalamic regions (dorsal, ventral, anterior, posterior, and center) from five medial-to-lateral brain levels were imaged at 40x magnification. After the red channel was cloaked to blind the observer to p-S6 levels, the green MAP-2 signal was used to manually outline the edges of clearly labeled neuronal cell bodies using Volocity's Freehand Tool. The Measure function was used to calculate the perimeter and area of all outlined cell bodies and was exported to Microsoft Excel for data analysis. After analysis, the red p-S6 channel was unmasked in order to sort cells into "p-S6 positive" and "p-S6 negative" cohorts, based on p-S6 immunolabeling intensity. Numbers of measured cells per cohort are indicated in Figure 3 and 5. Generalized Estimating Equations (log-normal generalized model) were used to compare genotypes with regards to neuronal size. Each mouse had multiple cells, which were treated as having correlated error. Cells were divided into those expressing pS6 and those not expressing pS6. Comparison between sizes of pS6-positive and pS6-negative cells within the knock-outs was a within-subjects comparison, while those between genotypes were between-subjects comparisons. Pair-wise comparisons were made using orthogonal contrast statements, with p-values adjusted using the Holm test to maintain family-wise alpha at 0.05.

Whole-cell Recordings

Slice Preparation: Brain sections were prepared from young mice (postnatal age: 20-23 days) of either sex as previously described (Kwiatkowski et al., 2002; Cruikshank et al., 2012). Briefly, mice were deeply anesthetized with isofluorane, then decapitated. The brains were quickly removed and placed in cold (4°C) oxygenated (5% CO_2, 95% O_2) slicing solution containing (in mM): 3.0 KCl, 1.25 NaH_2PO_4, 10.0 $MgSO_4$, 0.5 $CaCl_2$, 26.0 $NaHCO_3$, 10.0 Glucose, and 234.0 sucrose. Brains were then mounted, using a cyanoacrylate adhesive, onto the stage of a vibrating tissue slicer and horizontal brain slices (275-300 μm) containing the VB nucleus were obtained. Slices were immediately transferred to a holding chamber containing oxygenated, physiological saline solution maintained at 32±1°C. The oxygenated physiological solution (5% CO_2, 95% O2) contained (in mM): 126.0 NaCl, 3.0 KCl, 1.25 NaH_2PO_4, 2.0 $MgSO_4$, 2.0 $CaCl_2$, 26.0 $NaHCO_3$, and 10.0 glucose. After 15-20 min, the temperature was reduced to room temperature and the slices were allowed to incubate for an additional 60 min.

Whole-Cell Recording Procedure: Individual brain slices were placed in a submersion-type recording chamber maintained at 32±1ºC and continuously superfused (2.5-3 ml/min) with oxygenated physiological saline. VB neurons were visualized using a Zeiss Axioskop fixed-stage microscope equipped with IR-DIC optics and a water-immersion objective (40X, 0.75 NA, Zeiss). All but 6 mutant neurons were identified visually by expression of *R26*^{tdTomato}. Electrophysiological data were acquired using an Axoclamp-2B amplifier, filtered at 10 kHz and digitized at 20 kHz using a Digidata 1322A

digitizer in combination with pClamp10 software (Molecular Devices). For whole-cell recordings, patch pipettes had tip resistances of 3-6 MΩ when filled with a potassium-based internal solution containing (in mM): 130.0 K-gluconate, 4.0 KCl, 2.0 NaCl, 10 HEPES, 0.2 EGTA, 4.0 ATP-Mg, and 0.3 GTP-Tris, 14.0 phosphocreatine-K (pH 7.25, ~290 mOsm). During all recordings the pipette capacitance was neutralized and access resistance was continually monitored. Membrane potentials were not corrected for liquid junction potentials.

Data Analyses: Data were collected with protocols made with Clampex 10.0 and analyses were performed post-hoc using Clampfit 10.0. Resting membrane potentials (R_m) were measured within 2 min of break-in. Input resistances (R_{in}) were estimated as the slope of the voltage-current relationship obtained with current pulses (-50 to +50 pA, 25-50 pA increments, 800 ms duration). Membrane time constants (τ_m) were calculated from voltage responses to small negative current injections (3-5 pA, 500 ms duration). For τ_m, the voltage responses were fitted with a single exponential to the initial 150 ms of the responses. Input capacitances (C_{in}) were calculated as τ_m/R_{in}. Burst properties were characterized by holding the soma at a membrane potential of -60 mV with intracellular current and subsequently injecting large negative currents (400-1000 pA, 40-100 pA increments, 800 ms duration). When comparing low-threshold bursts, only trials in which the steady-state potential reached -70±2 mV were used. Tonic and single action potential properties were characterized by holding the soma at a membrane potential of -50 mV with intracellular current and injecting suprathreshhold positive current. Frequency-current relationships were obtained using large positive current injections (50-400 pA, 50 pA increments, 800 ms duration). Single action potential data were obtained by injecting the minimum current needed to elicit an action potential (10-200 pA, 10-15 pA increments, 800 ms duration). Action potential thresholds were calculated as the voltage difference between the steady-state potential and the point at which the rate of rise was greater than 15 mV/ms. Action potential amplitudes and half-widths were measured relative to threshold potential. After-hyperpolarizations (AHPs) were evoked by injecting a 2 ms suprathreshold positive current (600-1500 pA).

Generalized Hierarchical Linear Modeling was use to test for differential effects of *Tsc1* gene deletion at E12.5 and E18.5, while appropriately accounting for nested measurement of multiple cells within-mouse (up to 6 cells sampled in 12 mice for a total of 55). The choice of distribution on which the statistical model was based was chosen based on model diagnostic residual visualizations. Cell genotype and stage of tamoxifen were treated as fixed effects with cell genotype also treated as a random effect with a compound symmetry variance-covariance structure. Any model misspecification was adjusted for using classical sandwich estimation. Individual comparisons by cell genotype within tamoxifen time-points (i.e. $Tsc1^{\Delta E12/\Delta E12}$ mutants versus $Tsc1^{+/+}$ littermates) were made using orthogonal linear comparisons. The interaction effect of the omnibus represented the comparison of these effects.

In vivo Extracellular Recordings

Head-post Surgery and Craniotomy: Animals were anesthetized under 3.0% isoflurane (Isothesia, Butler Schein, Dublin OH) in O_2 within a plastic induction chamber and fitted into a stereotaxic apparatus (David Kopf Instruments, Tujunga CA). Throughout surgery, animals received 0.5-2.0% isoflurane in 1.0% O_2; levels were controlled with the use of an Isotec vaporizer (SurgiVet, Waukesha WI). Body temperature was maintained at 36-38°C with a heating pad (Cara, Inc., Warwick RI) during both surgery and recording sessions. Animals received 0.05 mL intraperitoneal injections of atropine sulfate (0.54 mg/mL, Med-Pharmex, Pomona CA) and buprenorphine hydrochloride (.03 mg/mL, Reckitt-Benckiser, Richmond VA), and a 0.025 mL intraperitoneal injection of dexamethasone (2 mg/mL, VEDCO, St. Joseph MO).

The dorsal surface of the head was shaved with a standard razor, and any residual fur was removed using a depilatory agent (Nair). Skull was exposed under aseptic conditions, and the center of the planned craniotomy was marked (AP: -1.2, L: 3.5). A custom-designed titanium head-post was affixed to the skull with C&B metabond (Parkell Inc., Edgewood NY) perpendicular to the sagittal plane. Posts can be clamped for quick and consistent head-fixing. Dental cement (Lang Dental, Wheeling IL) was

used to form a surface within the head-post interior for a saline well. The tissue surrounding the head-post was reattached to the head-post exterior edge using superglue (Loctite instant adhesive 454, Rocky Hill CT). An air-powered drill (Midwest Tradition Highspeed Handpiece, Dentsply Professional, Des Plaines IL) outfitted with a 0.5 mm regular carbide bur (Shank Type FGSS, Dentsply Professional) was used to clean away cement at the craniotomy site and thin the skull. The bone was removed, and the exposed brain was covered with saline. All recording equipment was secured onto a vibration isolation table (Technical Manufacturing Corporation, Peabody MA) to minimize noise and artifact. Animals were head-fixed, and anesthesia was maintained through infusion of 0.5-2.0% isoflurane through a nose cone; isoflurane levels were gradually lowered until the animal was just above the threshold at which there existed a paw pinch response.

NeuroNexus probes were used for all recording sessions. In some cases, bad contacts were present on probes, and these data were discarded. Local field potential (LFP) signals were sampled (30303 Hz), filtered (0.9 to 9000 Hz), and recorded using a Cheetah Data Acquisition System (NeuraLynx, Bozeman, MT). A four-axis micromanipulator (Siskiyou, Grants Pass OR) was used to clamp the probe, which was manually lowered to the brain surface. Prior to thalamic recordings, the probe angle was adjusted to approximately 25°. The probe was grounded on the head-post mount, and a reference wire was placed within the saline well. The probe was lowered at a controlled rate to depths of 1600µm or 2500µm for cortical and thalamic recordings, respectively. An air puffer, gated by a solenoid, was positioned above contralateral vibrissae and used to test for response to vibrissa deflection: application of such deflections was used to confirm electrode placement in SI and to ensure consistent quality of recording. After validation of probe location, ten minutes of baseline activity was recorded. A stimulus period consisting of 500 air puff trials followed; inter-trial periods were of randomly selected lengths between 2 and 8 seconds long, with a mean period of 5 seconds. At the end of the stimulus period, a 10 minute post-stimulus baseline period was recorded. Following recordings, the saline well was filled with a silicone elastomer (KwikCast, World Precision Instruments, Sarasota FL) to cap and protect the craniotomy between recording sessions. At the start of subsequent recording sessions, KwikCast was removed and the craniotomy area was inspected for bleeding, inflammation, and bone growth. Recordings then proceeded as previously described.

Recording Analysis: For each animal, a single SI recording session was selected for LFP analysis. The session chosen was that which exhibited the least clipping artifact and the highest amplitude responses following vibrissa deflection across the 16 probe channels. Within each chosen session, the contact exhibiting the largest amplitude and shortest duration responses following vibrissa deflection was identified as a putative layer IV contact and selected for analysis. The recorded signal from this contact was then low-pass filtered (0-150 Hz), downsampled (to 505.05 Hz), and clipping artifacts were removed.

Data from the entire recording session, including baseline (no stimulation) and vibrissa-stimulation periods, were analyzed using Matlab (MathWorks, Natick, MA). Each record was divided into 20-second non-overlapping time windows, and any trailing samples not included in these windows were discarded. The power spectral density (PSD) for each window was estimated using Welch's method (Matlab's `pwelch` command) with a 4096-point FFT, normalized by dividing by the sum of the PSD across all frequencies, and smoothed using a 5-pt moving average filter. For each animal, the average normalized PSD across the entire recording session was computed by taking the mean of the normalized PSDs across all the 20-second windows. Relative power at 3 Hz was calculated for each 20-second window by dividing the value of the normalized PSD at 3 Hz by the value at 1 Hz, and the average for each animal was taken to be the mean of this ratio across windows. For each animal, the number of 20-second windows in which normalized power at 3 Hz exceeded a threshold was then counted. This threshold was determined as the 97.5th percentile of normalized 3 Hz power across all animals. To test for significant differences between control and mutant subjects, two-tailed two-sample t-tests were performed by grouping all $Tsc1^{+/+}$ control animals (tamoxifen delivered at E12.5 and E18.5) and all mutant animals ($Tsc1^{\Delta E12/\Delta E12}$ and $Tsc1^{\Delta E18/\Delta 18}$), with a significance level, α, of 0.05.

Behavioral Analysis

Seizures and over-grooming: *Tsc1*$^{\Delta E12/\Delta E12}$ mice (n=11) and their littermate controls (*Tsc1*$^{+/+}$ or *Tsc1*$^{fl/fl}$, n=19; *Tsc1*$^{+/\Delta E12}$ n=17) were videotaped in their home cage using a digital camera for 8-minute epochs 2-3 times per week between 2 months of age and 8 months of age. Two *Tsc1*$^{\Delta E12/\Delta E12}$ mice died prematurely of unknown causes and were not included in the behavioral analysis. *Tsc1*$^{\Delta E18/\Delta E18}$ mice (n=17) and their littermate controls (*Tsc1*$^{+/+}$ or *Tsc1*$^{fl/fl}$, n=25; *Tsc1*$^{+/\Delta E18}$, n=6) were observed once per week for 8 minutes, beginning at 2 months of age and continuing through 8 months of age. Videos were analyzed by an observer who was blinded to animal genotypes. Number and duration of all seizures and self-grooming behaviors were manually tallied (grooming events lasting less than 1 second were rounded up to 1 second duration). An independent observer tallied a subset of videos, and the two observers' tallies had a high level of concordance, confirming the reproducibility of the manual data analysis approach. Animals were euthanized for humane reasons by intracardiac perfusion if they developed severe grooming lesions. Data was analyzed in Excel (Microsoft) and plotted using KaleidaGraph (Synergy). Generalized Estimating Equations were used to compare genotypes with regards to percent minutes grooming (binomial generalized model grooming/total minutes) and seizure event rates (negative-binomial generalized model offset by log total hours). Comparisons represented between-subjects comparisons, with multiple observations within an animal modeled as having correlated error. Pair-wise comparisons were made using orthogonal contrast statements, with p-values adjusted using the Holm test to maintain family-wise alpha at 0.05.

Von Frey Filament test: Withdrawal thresholds from mechanical stimuli of von Frey filaments of ascending bending force (from 0.008 to 300g of force) were applied five times to the plantar surface of the bilateral hind paws. A positive response was defined as withdrawal from the von Frey filament on at least 3 of the 5 contacts. Confirmation of threshold was then tested by examining the filament above and below the withdrawal response. Significance was assessed by a one-tailed two-sample t-test, α=0.05.

Hot plate test: The test was based on that described by Eddy and Leimbach (1953). A glass cylinder (16 cm high, 16 cm diameter) was used to keep the mice on the heated surface of the plate, which was kept at a temperature of 53C +/-0.2°C (Ugo Basile model 7280). The first of two nociceptive thresholds were evaluated: licking of the hind paw or sustained (> 1s) lifting of the hind paw from the surface. The cut-off for a response was 40 s at which point the trial was terminated. Significance was assessed by a one-tailed two-sample t-test, α=0.05.

Wire Hang test: Mice were placed on a wire cage lid, which was then inverted gently 180deg so that the mouse gripped the wire at a distance of ~16cm above the floor of an empty cage. Latency to fall was recorded, with a cut-off time of 300 s. Animals were provided with 4 opportunities to perform on this task and the longest duration to fall was collected. Significance was assessed by a one-tailed two-sample t-test, α=0.05.